Ann. Geophys., 24, 2719–2733, 2006
www.ann-geophys.net/24/2719/2006/

Annales Geophysicae

Evidence of standing waves during a Pi2 pulsation event observed on Cluster

A. B. Collier[1,2], **A. R. W. Hughes**[1], **L. G. Blomberg**[2], **and P. R. Sutcliffe**[3]

[1]School of Physics, University of KwaZulu-Natal, Durban, South Africa
[2]Dept. of Space and Plasma Physics, School of Electrical Engineering, Royal Institute of Technology, Stockholm, Sweden
[3]Hermanus Magnetic Observatory, Hermanus, South Africa

Received: 11 April 2006 – Revised: 16 August 2006 – Accepted: 31 August 2006 – Published: 20 October 2006

Abstract. Observations of Pi2 pulsations at middle and low latitudes have been explained in terms of cavity mode resonances, whereas transients associated with field-aligned currents appear to be responsible for the high latitude Pi2 signature.

Data from Cluster are used to study a Pi2 event observed at 18:09 UTC on 21 January 2003, when three of the satellites were within the plasmasphere (L=4.7, 4.5 and 4.6) while the fourth was on the plasmapause or in the plasmatrough (L=6.6). Simultaneous pulsations at ground observatories and the injection of particles at geosynchronous orbit corroborate the occurrence of a substorm.

Evidence of a cavity mode resonance is established by considering the phase relationship between the orthogonal electric and magnetic field components associated with radial and field-aligned standing waves. The relative phase between satellites located on either side of the geomagnetic equator indicates that the field-aligned oscillation is an odd harmonic. Finite azimuthal Poynting flux suggests that the cavity is effectively open ended and the azimuthal wave number is estimated as $m\sim$13.5.

Keywords. Magnetospheric physics (MHD waves and instabilities; Plasmasphere; Storms and substorms)

1 Introduction

Pi2 pulsations are damped Ultra Low Frequency (ULF) waves generally characterised by an abrupt commencement followed by a decay in amplitude which typically only endures for a few cycles. Categorised as irregular pulsations (Jacobs et al., 1964), Pi2 have periods between 40 and 150 s. Some Pi2 are unequivocally the result of the onset or intensification of the substorm expansion phase (e.g., Rostoker, 1967a), while others have been recorded during periods without substorm activity (Sutcliffe, 1998; Kim et al., 2005).

Pi2 are most frequently observed close to the midnight meridian between 20:00 and 24:00 LT (Sutcliffe, 1975). Maximum amplitudes are found in the auroral zone (Akasofu, 1968; Saito, 1969), while a secondary amplitude peak has been noted in the vicinity of the plasmapause (Gupta and Stening, 1971; Stuart, 1974; Saito et al., 1976).

The characteristics of Pi2 pulsations observed at high latitudes are quite distinct from those at middle and low latitudes, and it is thus commonly believed that they are generated by different mechanisms (Gupta and Stening, 1971; Olson, 1999). While the pulsations are well defined at lower latitudes, closer to the poles they are irregular and complex, contaminated by a pronounced level of background noise, particularly in the Pi1 band (Stuart and Booth, 1974; Rostoker and Olson, 1978; Southwood and Stuart, 1980). Yeoman et al. (1991) showed that Pi2 are predominantly transverse at auroral latitudes and compressional at lower latitudes. At high latitudes Pi2 are encountered exclusively in a limited range of local times around magnetic midnight corresponding roughly to the extent of the substorm current wedge (Singer et al., 1983). At middle and low latitudes they are found simultaneously, with similar frequency spectra, at essentially all local times (Sutcliffe and Yumoto, 1989, 1991). Although Pi2 pulsations on the dayside are often obscured by signals from other sources, numerous observations of dayside Pi2 have been made over a range of latitudes straddling the geomagnetic equator (Stuart and Barsczus, 1980; Sutcliffe and Yumoto, 1989, 1991). The detection of Pi2 on the dayside, when their source is clearly around midnight, implies the involvement of fast mode waves propagating across the ambient magnetic field.

Pi2 are produced during the expansion phase onset by the rapid reconfiguration of the magnetotail (Shiokawa et al., 1998). The induced azimuthal electric field resulting from the dipolarisation of distended magnetic field lines in the tail

Correspondence to: A. B. Collier
(colliera@ukzn.ac.za)

Published by Copernicus GmbH on behalf of the European Geosciences Union.

causes high-speed earthward $\boldsymbol{E}\times\boldsymbol{B}$ flow. The flow is decelerated and diverted when it encounters the boundary between dipolar and tail-like magnetic field lines, leading to the formation of the substorm current wedge (SCW). The transients associated with the initiation of and subsequent fluctuations in the field-aligned currents may lead to the high-latitude Pi2 signature (Sakurai and McPherron, 1983; Baumjohann and Glaßmeier, 1984). Compressional waves generated by the impact of the injected plasmasheet particles on dipolar magnetic field lines propagate across the field lines into the inner magnetosphere where they cause Pi2 at lower latitudes.

Observations of Pi2 over a range of middle and low latitudes often display one or several discrete frequencies. These uniform spectral features have been attributed to transient surface waves propagating on the plasmapause (Sutcliffe, 1975; Southwood and Stuart, 1980), or temporal fluctuations of bursty bulk flows with similar spectral content (Kepko and Kivelson, 1999). However, the most established explanation invokes cavity or fast mode resonances (FMRs), which are compressional waves trapped in cavities formed within the magnetosphere (Lin et al., 1991; Sutcliffe and Yumoto, 1991; Takahashi et al., 1995; Allan et al., 1996; Pekrides et al., 1997).

In principle the magnetosphere can be represented by a pair of coupled cavities separated by the plasmapause (Allan et al., 1986; Zhu and Kivelson, 1989). The inner radial boundary arises from the Alfvén speed gradient, while the outer boundary occurs at the magnetopause. The substorm plasma injection front may also establish a boundary on the nightside (Lin et al., 1991). Although the source of fast mode waves may be impulsive and broadband, discrete frequencies are selected which match the eigenfrequencies of the cavities. The spectrum of resonant cavity mode waves therefore corresponds to those frequencies for which a standing wave may form between the inner and outer radial boundaries. Since these resonant frequencies are determined by the geometry of the cavity as a whole, they do not vary with L.

Although the magnetosphere is closed on the dayside, it is elongated in the antisunward direction to form the magnetotail. This asymmetrical azimuthal geometry is more reminiscent of a waveguide or open-ended cavity (Walker et al., 1992). Waters et al. (2002) observed that the formation of radial resonant structures is more likely on the dayside, where reflection occurs at the magnetopause, whereas on the nightside the lack of a well defined boundary outside the plasmapause may preclude the occurrence of outer cavity modes, and FMRs may simply be confined within the plasmasphere. The numerical results of Lee (1996) indicate that plasmaspheric cavity modes may exist in the absence of an outer magnetospheric boundary. However, they caution that since the boundary presented by the plasmapause has only finite width, energy can tunnel through it into the outer magnetosphere. The eigenfrequencies of the fundamental and second harmonic plasmaspheric cavity modes are in the intervals 10 to 15 mHz and 26 to 28 mHz respectively (Lee, 1998).

The high coherence observed between compressional oscillations in the plasmasphere and at low latitudes on the ground supports the plasmaspheric origin of low latitude Pi2 pulsations (Takahashi et al., 1995, 2003). The observed increase of the average Pi2 frequency with geomagnetic activity (Rostoker, 1967b) also substantiates the cavity resonance model: during periods of enhanced activity the size of the plasmasphere is reduced and the cavity mode frequencies are thus elevated (Takahashi et al., 2003).

Beyond the limits of the cavity the compressional mode decays exponentially but may still couple to the toroidal mode to form field line resonances (FLRs). Pi2 polarisation displays a pronounced variation with latitude (Fukunishi, 1975). The latitude at which the sense of polarisation reverses coincides with a maximum in the toroidal mode amplitude (Samson et al., 1971; Lanzerotti et al., 1974). This suggests that the maximum is associated with a FLR. Takahashi et al. (1995) failed to find evidence of FLRs during Pi2 at $L<5$, but Keiling et al. (2001) were able to identify a pair of Pi2 events with FLR signatures.

2 Instrumentation, data and analysis

The Cluster constellation of four satellites (Escoubet et al., 2001) was launched during the year 2000 into a nearly polar orbit with inclination $\sim$88.5°, apogee 19.4 R_E, perigee 4.2 R_E and eccentricity 0.64. The orbit has a period of 57.1 h, of which an average of only 100 min are spent in the inner magnetosphere ($L<6$). Critically, under moderate geomagnetic conditions, the orbit regularly brings the satellites into the plasmasphere. Around 25% of the forays into the plasmasphere occur between local times of 21:00 and 03:00.

The orientation of the Cluster orbital plane remains fixed in inertial space. Consequently the local time of perigee varies with the season, proceeding from noon on 2 September to midnight on 30 April. Since Pi2 are most clearly observed at low invariant latitudes around midnight, the most favourable period for identifying these events on Cluster is during the northern hemisphere winter. The search for Pi2 events was therefore focused on intervals during this period when the constellation was at low L on the nightside. Several events were identified, but too few for a reasonable statistical appraisal. An intriguing instance, during which only three of the satellites were located within the plasmasphere, is presented here as a case study. Three other promising events were also considered in detail and will be discussed in a forthcoming publication.

Pulsation data were obtained from the Electric Field and Wave (EFW) (Gustafsson et al., 1997) and Fluxgate Magnetometer (FGM) (Balogh et al., 1997) instruments on Cluster. The EFW experiment has two pairs of spherical probes, each sensor deployed at the end of a wire boom in the spin plane of the satellite. The FGM instrument is

a tri-axial fluxgate magnetometer measuring the complete magnetic field vector.

The Cluster electric and magnetic field data are originally presented in Geocentric Solar Ecliptic (GSE) coordinates. The spin axes of the satellites are perpendicular to the GSE $X-Y$ plane, and the spin period is 4 s. The spin-averaged data therefore have a nominal sampling rate of 250 mHz. The resulting Nyquist frequency of 125 mHz is quite adequate for the phenomena under consideration. Since the time series from the four satellites are not synchronised, the data were linearly interpolated onto a common time base.

The EFW instrument only supplies data for the two components of the electric field in the spin plane of the satellite, which is effectively the ecliptic plane. However, the MHD condition which precludes the existence of an electric field parallel to the ambient magnetic field may be applied to estimate the third component. This procedure is only reliable when the magnetic field does not lie too close to the ecliptic plane, and in practice is only applied when it is inclined at an angle of at least 10° above or below the ecliptic.

The analysis of ULF pulsation data in space is conveniently undertaken in the mean field-aligned (MFA) coordinate system (ν, ϕ, μ), for which $\hat{\boldsymbol{\mu}}$ is parallel to the mean background magnetic field, $\hat{\boldsymbol{\phi}}$ is directed azimuthally eastward, and $\hat{\boldsymbol{\nu}}$, which completes the right-handed orthogonal triplet, is perpendicular to the field line pointing outward. The unit vectors are defined as $\hat{\boldsymbol{\mu}}=\boldsymbol{B}/|\boldsymbol{B}|$, $\hat{\boldsymbol{\phi}}=\hat{\boldsymbol{\mu}}\times\boldsymbol{r}/|\hat{\boldsymbol{\mu}}\times\boldsymbol{r}|$, where $\boldsymbol{r}$ is the geocentric position vector, and $\hat{\boldsymbol{\nu}}=\hat{\boldsymbol{\phi}}\times\hat{\boldsymbol{\mu}}$.

The background magnetic field used to effect the transformation to MFA coordinates is calculated as a 20 min running average of the FGM data. Conversion therefore removes all perturbations with periods greater than 1200 s. In the MFA coordinate system the magnetic field perturbation consists of the compressional, b_μ, radially transverse, b_ν, and azimuthally transverse, b_ϕ, components. The b_μ and b_ν components constitute the poloidal mode, while the toroidal mode only involves b_ϕ.

A significant advantage of wave studies carried out with multiple satellites is the ability to discern the spatial and temporal components of an oscillation. Such an analysis is conveniently performed in the frequency domain. In order to obtain a reliable estimate of the phase difference between a wave at two distinct locations, or indeed between two components of a wave at a single location, one should first establish whether the two waveforms have a stable phase relationship. This may be assessed from the coherence spectrum,

$$\gamma^2 = \frac{|S_{ij}|^2}{S_{ii}S_{jj}}, \tag{1}$$

where S_{ii} and S_{jj} are the power spectral densities of the two waveforms, and S_{ij} is the cross-power spectral density (CPSD) (Paschmann and Daly, 1998). The coherence expresses the correlation between the two signals as a function of frequency. It can be shown that $0\leq\gamma\leq1$, where an appreciable value for γ indicates that the two signals have a consistent phase relationship and correspond to an ordered wave rather than simply arising from stochastic noise. A coherence threshold of 75% was imposed in this analysis. For frequencies where γ exceeds this threshold the phase difference between the waveforms may be reliably determined from the ratio of the imaginary and real parts of S_{ij},

$$\tan\delta = \frac{\Im\{S_{ij}\}}{\Re\{S_{ij}\}}. \tag{2}$$

When the phase difference is averaged over a range of frequencies, only those frequencies which surpass the coherence threshold are considered and the magnitude of S_{ij} is used as a weighting factor. The notation $\delta(\cdot\,,\cdot)$ is used to indicate the phase difference between two waveforms, where the first argument specifies the reference waveform. For example, $\delta(E_\phi, b_\mu)$ designates the phase of b_μ relative to E_ϕ.

The fact that Pi2 pulsations are transient phenomena is not strictly conducive to the application of the spectral techniques described above, which present an average over the time interval to which they are applied. A more appropriate technique involves the use of complex demodulation to determine the instantaneous amplitude and phase of the signals. The waveforms are first filtered over the Pi2 band before the analytical signal is calculated. This facilitates the estimation of instantaneous cross-spectral parameters (Webb, 1979).

3 Event description

On 21 January 2003 the expansion phase of a substorm commenced at approximately 18:09 UTC. The beginning of the associated Pi2 pulsation envelope observed on the ground was taken to be the onset time.

3.1 Auxiliary data

Los Alamos National Laboratory (LANL) geostationary electron flux data are presented in Fig. 1. The nominal substorm onset time is identified in this and all subsequent plots by a vertical grey line. A dramatic enhancement of the electron flux at the satellite situated closest to midnight, LANL-97A, occurs shortly after substorm onset. The dispersionless injection of plasma into the nightside inner magnetosphere is an acknowledged signature of the substorm expansion phase (McIlwain, 1974). The injected electrons are subsequently detected with progressively greater dispersion by satellites located at later local times. Fluctuations in the flux measured at 1990-095, located near the dusk meridian, occur roughly 30 min after the injection. These oscillations have a period of around 250 s, which places them in the Pc5 range. Their occurrence corresponds to the arrival of the injected electrons at 1991-080, situated around dawn. It is thus possible that the fluctuations are produced by the drift-bounce resonance instability associated with velocity-dispersed ions injected

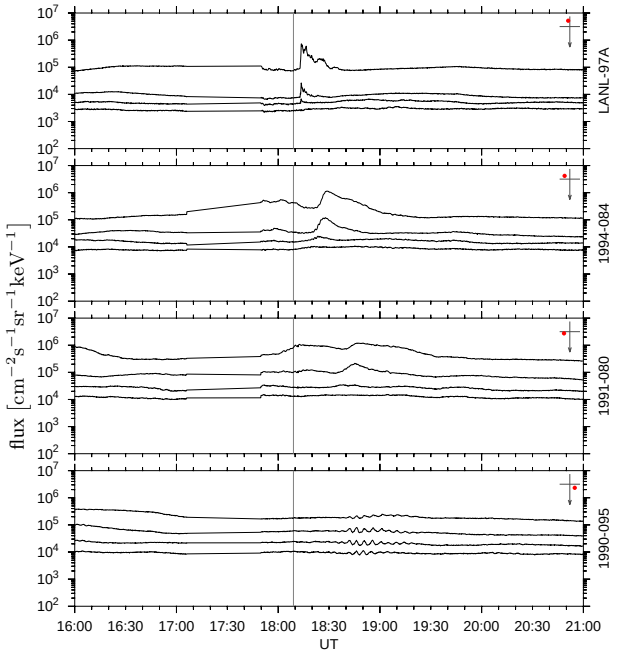

Fig. 1. Electron flux data for 21 January 2003 from Synchronous Orbit Particle Analyzer (SOPA) instruments on LANL geosynchronous satellites. The four traces in each panel represent different energy channels; from top to bottom they are 50–75, 75–105, 105–150 and 150–225 keV. In the upper right corner of each panel is an inset indicating the local time of the satellite at the event epoch (the arrow points sunward).

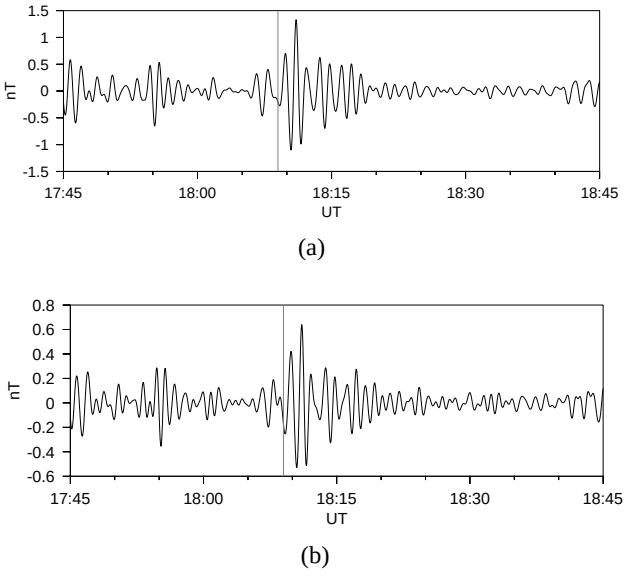

Fig. 2. Perturbations in the H component of the magnetic field at ground stations **(a)** Yinchuan [YCB] and **(b)** Kakioka [KAK]. The waveforms are bandpass filtered over the Pi2 frequency range.

during the substorm onset, and which would have reached 1990-095 at about this time (Glassmeier et al., 1999). Unfortunately no proton flux data are available for this period on 1990-095 to confirm or refute this proposition.

The magnetic perturbations at two northern hemisphere ground stations, Yinchuan (38.5° N 106.3° E GEO, L=1.43) and Kakioka (36.2° N 140.2° E GEO, L=1.32), are plotted in Fig. 2. At the time of the event the local times at these two stations were 01:14 and 03:29 respectively. They were thus well situated for the observation of Pi2 pulsations. At both locations Pi2 activity was initiated by a strong impulse at 18:09 UTC.

3.2 Cluster data

At the moment of substorm onset Cluster's centroid was below the geomagnetic equatorial plane in the midnight-dawn quadrant (02:40 MLT) at a geocentric distance of 4.4 R_E. Table 1 presents the GSE coordinates, McIlwain's (1961) L parameter, magnetic latitude, magnetic local time and relationship to the plasmasphere for each of the satellites during the event. The constellation assumed a sparse configuration with a mean separation of 9900 km. Whereas C1, C2 and C4 were situated at L<5, C3 was at L=6.6. C3 was moving towards lower L, while the rest were close to perigee.

Table 1. Location of the Cluster satellites during the event on 21 January 2003, given in Cartesian GSE coordinates [distances measured in Earth radii, R_E], McIlwain's (1961) parameter, magnetic latitude (λ) and magnetic local time (MLT). Positions were transformed from GSE to Solar Magnetic (SM) coordinates and a centred dipole magnetic field was assumed when calculating L, λ and MLT. The position of each satellite with respect to the plasmasphere is indicated symbolically (×= inside plasmasphere; |= on plasmapause; ○= outside plasmasphere).

	X	Y	Z	L	P/S	λ	MLT
C1	–3.606	–3.023	0.371	4.7	×	1.9°	02:38
C2	–3.318	–2.932	–0.253	4.5	×	–5.9°	02:34
C3	–2.475	–3.305	–2.168	6.6	○	–32.7°	02:44
C4	–2.759	–2.991	–0.944	4.6	×	–17.0°	02:43

Furthermore, while C3 was at a relatively high magnetic latitude, the remaining satellites were at lower λ, with C1 and C2 closely bracketing the magnetic equatorial plane. The entire constellation was moving northward.

Entry into the plasmasphere may be gauged by reference to the EFW probe potential, as well as by consulting the RAPID omnidirectional electron flux and CIS proton density, although the latter instruments are saturated in the radiation belts and the data are thus contaminated (H. Rème, personal communication, 2006). EFW probe potential, plotted in Fig. 3, provides an indication of the plasma density in the vicinity of the satellites. Prior to around 12:00 UTC the

constellation was located outside the magnetosphere on the dayside, which accounts for the elevated potential produced by the heightened density of the solar wind plasma. At the time of the event all satellites except C3 had already entered the plasmasphere. The potential on C3 was still growing during the event, indicating that it was likely to have been in the plasmatrough or in the process of traversing the plasmapause. Entry and exit from the plasmasphere are most apparent on C1 and C2. The Active Spacecraft Potential Control (ASPOC) was activated at 20:00 and 19:30 UTC on C3 and C4 respectively, which conceals their exit from the plasmasphere.

The filtered Cluster electric and magnetic field waveform data are plotted in Fig. 4. The data were bandpass filtered over the Pi2 period range. The filter was applied in both the forward and reverse directions to remediate phase distortion. The interval used later for spectral analysis is delimited by vertical dashed lines. Electric field data are not available in MFA coordinates for C3 during the event since the background magnetic field direction was passing through the spin plane of the satellite. Clear Pi2 pulsations with comparable amplitudes are evident on C1, C2 and C4. The pulsations appear to be divided into two distinct packets, the first of which has both larger amplitude and longer duration. These packets are also apparent in the ground data presented in Fig. 2. This structure suggests either two distinct Pi2 events or the beating of two closely spaced frequencies. On C1 the magnetic perturbation is confined to the compressional component, with peak amplitude 0.2 nT, while C2 and C4 experience significant toroidal oscillations, with peaks in b_ϕ of 0.5 nT and 1.1 nT, respectively. The variation of the electric field is predominantly in E_ν, with a peak amplitude of around 2.2 mV/m on all three satellites within the plasmasphere. The dominance of E_ν implies either a compressional mode propagating azimuthally or a transverse mode propagating along the magnetic field. The waveforms represent a transition between poloidal and toroidal modes: whereas at C1 the wave is principally compressional, at C4 the azimuthal component is prevalent; at C2 waves of comparable amplitude are present in both toroidal and poloidal components.

Although pulsation activity certainly exists at C3, its onset precedes the activity at the other satellites and its form is highly irregular, quite distinct from the symmetric envelopes on the remaining satellites. It is reasonable to conclude that the dynamics of the Pi2, if observed on C3, differ significantly from those on the other spacecraft. One cannot, however, exclude the possibility that other waves with similar spectral content mask the event at C3. During the 15 min prior to the start of the event C3 traversed an earthward field-aligned current system, which produced a characteristic dipolar signature in the absolute FGM data. The perturbations reflected in Fig. 4c may in part be due to these field-aligned currents.

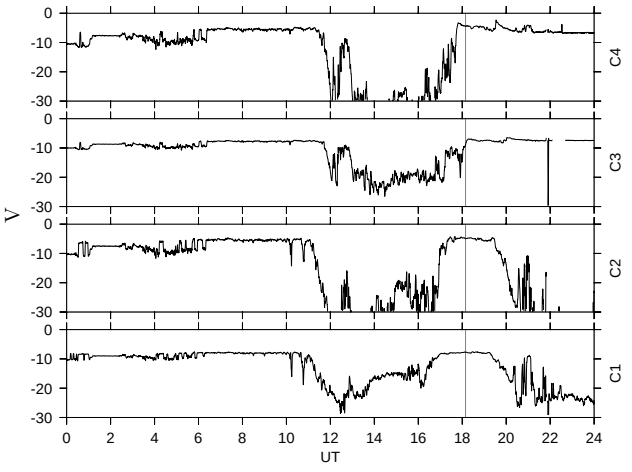

Fig. 3. EFW probe potential on 21 January 2003.

Despite the dominance of the toroidal component at C3, some level of coupling to the poloidal mode must occur since such high latitude pulsations should have $m \neq 0$ in order to be confined to the longitudinal extent of the SCW. Consideration of the instantaneous cross-power spectral density data for the Pi2 band plotted in Fig. 5 indicates that there is a high degree of correlation between the meridional and azimuthal magnetic field oscillations during the event, while there is less coherent activity either before or after this period. This suggests that some pulsation activity at C3 is indeed associated with the substorm. The coherent oscillations in b_ϕ and b_ν, where the former has a substantially larger amplitude, is suggestive of a FLR, where the compressional oscillation excites a resonant response and feeds power into the transverse oscillation (Chen and Hasegawa, 1974). Moreover, since C3 is located at L=6.6, it lies on a field line which maps down to the auroral zone, where the elevated ionospheric conductivity is conducive to the formation of a FLR. The relative phase is somewhat erratic during the event, suggestive of a bursty process with numerous phase skips. This irregularity is also reflected in the amplitude of the CPSD.

The observations described above are similar to the measurements of Kim et al. (2001), who found Pi2 events identified by compressional oscillations within the plasmasphere and transverse oscillations at geosynchronous orbit. Osaki et al. (1998) contended that the compressional component of Pi2 within the plasmasphere may be limited to magnetic latitudes $|\lambda| \lesssim 20°$, however, the locations of the Cluster satellites during the event on 21 January 2003 preclude the evaluation of this hypothesis.

Figure 6 shows the magnetic field power spectral density (PSD) at each of the satellites. The PSD estimates were computed using Welch's (1967) method. Data from the maximum entropy method (MEM) are also included since these provide improved frequency resolution for a sample of fixed duration (Sutcliffe, 1974), and are used to determine the peak

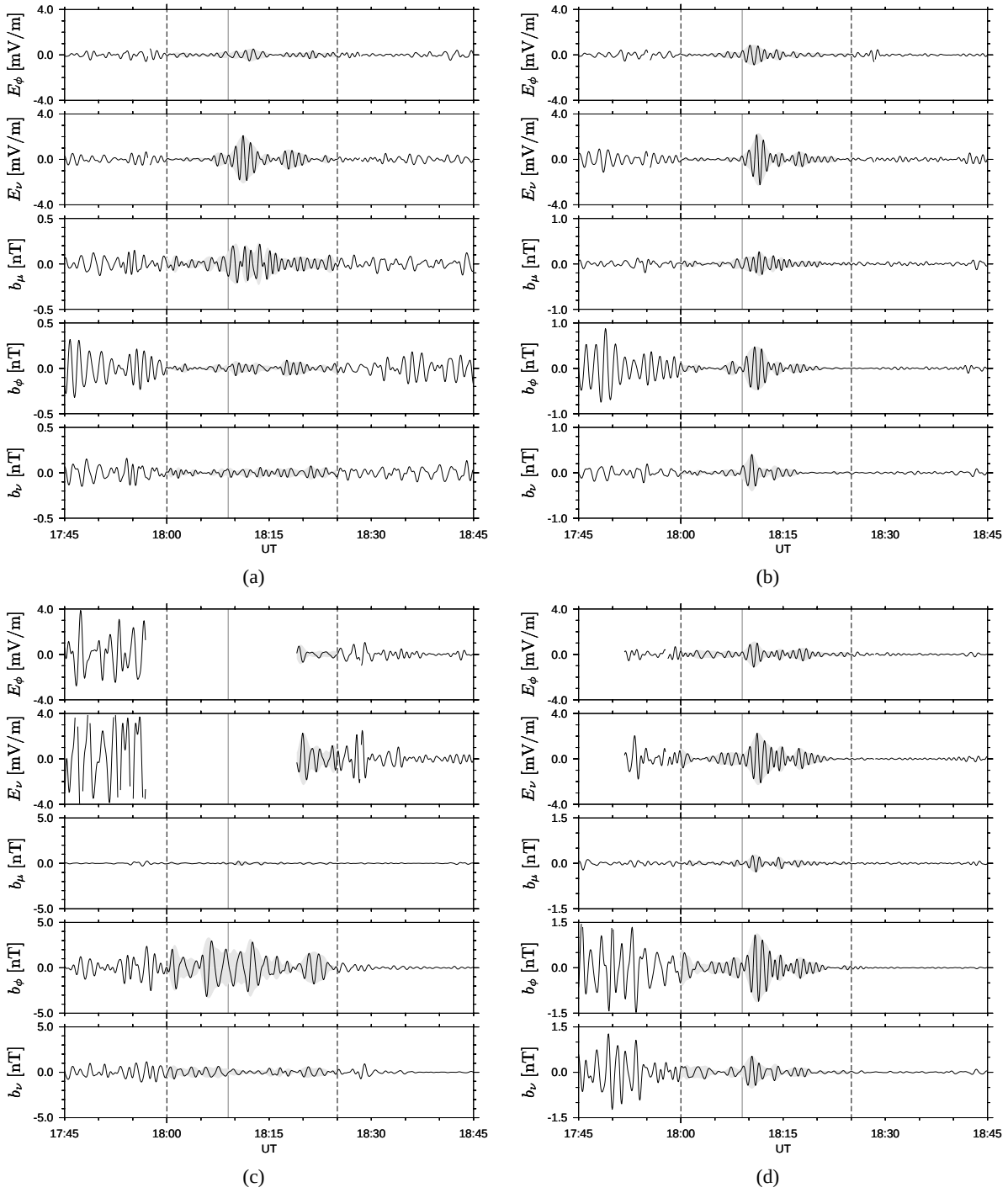

Fig. 4. EFW and FGM waveforms for 21 January 2003 on **(a)** C1 [Rumba], **(b)** C2 [Salsa], **(c)** C3 [Samba] and **(d)** C4 [Tango]. The signals have been bandpass filtered to extract periods in the range 40–150 s. The gaps in the EFW data for C3 and C4 occur where it was not feasible to apply $\boldsymbol{E}\cdot\boldsymbol{B}$=0, and transformation of the electric field to MFA coordinates was thus impossible.

frequencies. Since the spectral power decreases rapidly with frequency, the data have been pre-whitened by taking the first difference of the waveform. The spectral peaks for the azimuthal magnetic field on C1, C2 and C4 are at 17.2, 17.0 and 16.0 mHz respectively. The small differences in the frequencies of these peaks are probably not significant in view of the brief duration and damped form of the pulsations. The azimuthal spectrum at C3 is broadband with little evidence of preferred frequencies. This might appear to contradict the suggestion of a FLR at C3, but since the satellite is located near to the plasmapause it is exposed to a broad range of FLR frequencies, any or all of which may be excited. Olson and Rostoker (1975) found that spectra near the auroral electrojet were spread over a wide range of frequencies.

The compressional spectrum on C3 contains a peak at 15.5 mHz, but it is both wide and of low amplitude. On the other three satellites there is clear evidence of enhancement in $S_{\mu\mu}$ at a sequence of discrete frequencies which are likely to correspond to the fundamental and higher harmonics of a cavity mode resonance.

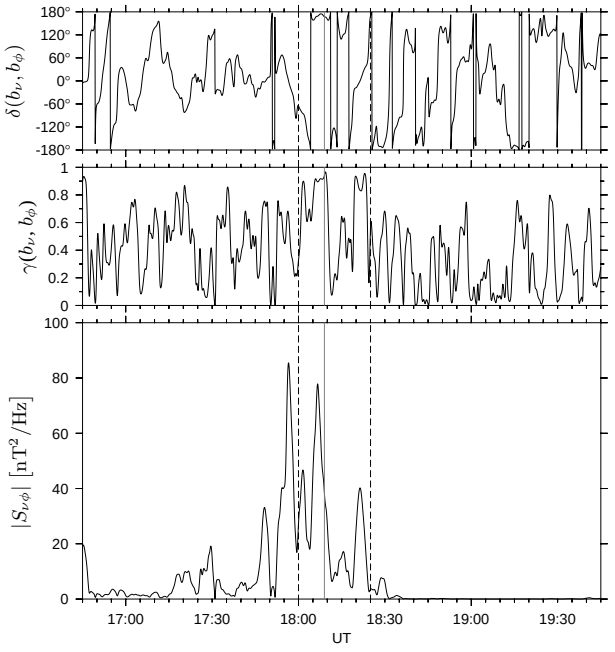

Fig. 5. Instantaneous amplitude and phase of the (b_ν, b_ϕ) cross-power spectral density averaged over the Pi2 band on C3.

4 Discussion

Various aspects of the event are now examined in greater detail. Specifically, evidence for cavity mode and field line resonances is considered, the azimuthal wave number is estimated, and the magnitude and orientation of the Poynting vector are discussed.

The normal modes of the magnetospheric cavity have both the meridional and field-aligned components of the wave vector quantised such that the total phase change along a return path across the cavity in either the ν or μ direction is an integral multiple of 2π. Depending on whether the cavity is open or closed in the azimuthal direction (in the former case the waveguide description applies), the azimuthal wave number may either assume arbitrary values or be restricted to discrete allowed values. The existence of a waveguide mode may be verified by establishing that the waves are standing in both the radial and field-aligned directions. If, in addition, it can be shown that there is no azimuthal propagation, then the conditions for a closed cavity mode have been satisfied.

A wave propagating in the radial direction involves the azimuthal electric field and compressional magnetic field. A standing wave should be identified by $\delta(E_\phi, b_\mu)=\pm 90°$ (Chi and Russell, 1998; Takahashi et al., 2001; Waters et al., 2002), while $\delta(E_\phi, b_\mu)=0°$ or $\pm 180°$ are consistent with a travelling wave. Equivalently, the cosine of the phase difference may be used, where $\cos\delta=0$ corresponds to a standing wave, while $\cos\delta=\pm 1$ indicates a propagating wave. Furthermore, the parameter $\cos\delta$ may also be used to estimate reflection coefficients (Potemra et al., 1989). Keiling et al. (2001) successfully applied these criteria to data from the Polar satellite.

For the event on 21 January 2003 the b_μ and E_ϕ oscillations were coherent at each of the satellites located within the plasmasphere. Table 2a reflects the mean phase differences calculated by averaging over those frequencies for which the coherence threshold was exceeded. The values of $\delta(E_\phi, b_\mu)$ are all close to $\pm 90°$. To illustrate the source of the data in Table 2a, the coherence and phase at each of the satellites are plotted in Fig. 7. The coherence exceeds the threshold within the Pi2 band at all satellites, but whereas the coherent range of frequencies is consistent between C2 and C4, it differs at C1. The phase difference of $93.4° \pm 1.7°$ at C1 appears to provide the most compelling evidence of a radial standing wave. At the remaining satellites the phase differences indicate that the compressional magnetic field and azimuthal electric field are not quite in quadrature (the absolute phase differences are within $\sim 25°$ of $90°$), and imply a superposition of standing and propagating waves, indicating imperfect reflection at the radial boundaries.

The plots of phase versus time in Fig. 7 correspond to the phase difference between the analytical signals, which are bandpass filtered over the Pi2 range. An examination of the instantaneous phase illustrates that the averaged data in Table 2a should be treated with caution. Although the phase at C4 fluctuates somewhat erratically during the event, its mean is around $-90°$ with a transitory departure at approximately 18:15 UTC induced by the transition between the two wave packets. The phase at C2 exhibits a greater degree of variability: periods of around $\pm 180°$ are interspersed between intervals of roughly $-45°$. The data at C1, however,

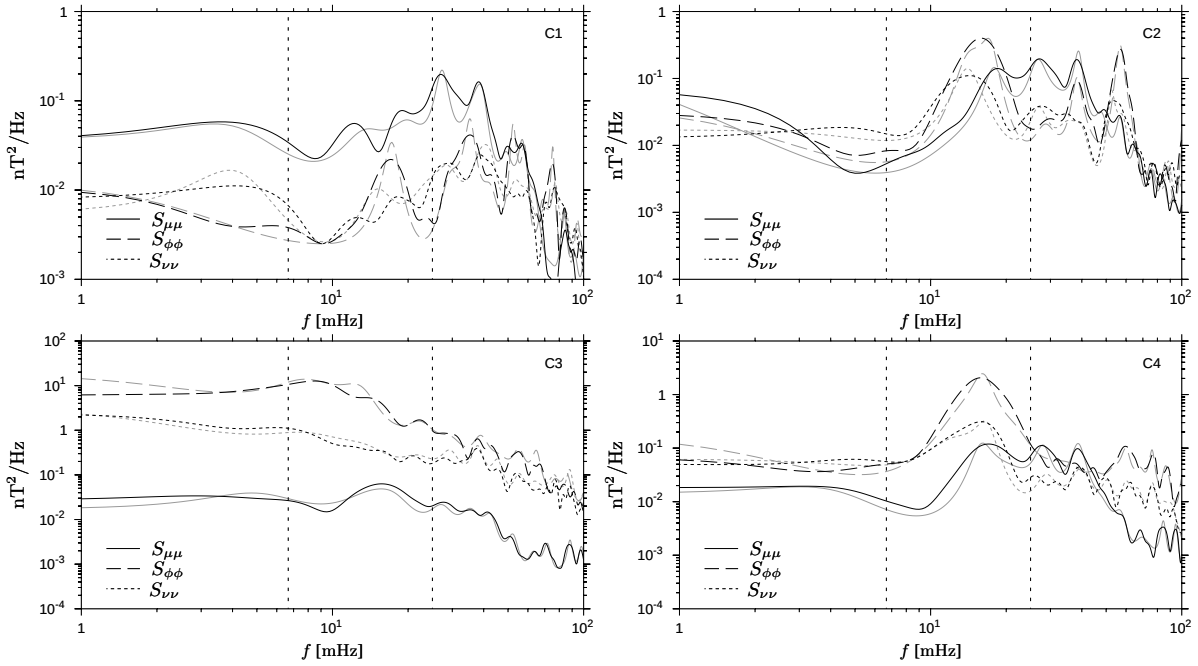

Fig. 6. Power spectral densities of the magnetic field components for the interval 18:00 to 18:25 UTC on 21 January 2003. The black curves correspond to the PSD calculated using Welch's method, while the grey curves were obtained using the MEM. The Pi2 band (6.7–25.0 mHz) is enclosed between the vertical dashed lines.

display a wide range of phase, progressing from 90° to −90°. Thus, although C1 presented the most convincing argument for a cavity resonance on the basis of cross-spectral analysis, closer examination reveals that the average cross-phase does not provide an adequate reflection of the true phase relationship. The misleading results for C1 may be attributed to the various phase skips in b_μ evident in Fig. 4a , which account for the deficient coherence in the upper portion of the Pi2 band. Those frequencies which are sufficiently coherent correspond to the lower frequency peak evident at C1 in Fig. 6, but which does not appear at the other two satellites.

In a simplistic model of the plasmasphere, where the magnetic field and plasma density are assumed to be uniform, the fundamental cavity resonance has a compressional magnetic field node located midway between the plasmapause and the inner boundary (Takahashi et al., 1995). In a more realistic model the compressional node is shifted outward, and may lie close to the plasmapause (Takahashi et al., 2003). The relative phase of E_ϕ and b_μ is reversed across the compressional node, with E_ϕ leading b_μ outside the node. The credible phase differences at C2 and C4 are consistent with locations outside the compressional node. Nodes also exist in the azimuthal electric field on the radial boundaries. The relatively weak E_ϕ amplitude at C1, which is located at the largest L of those satellites within the plasmasphere, conforms to a fast mode standing wave with an azimuthal electric field node in the vicinity of the satellite.

The case for a cavity mode resonance may be reinforced by considering the radially transverse magnetic perturbation. The field-aligned portion of the poloidal mode is comprised of the meridional magnetic and azimuthal electric fields. Their mean relative phase is given in Table 2b, where it is apparent that at both C2 and C4 the phase difference is approximately −90°. The variation of the phase as a function of time and frequency is displayed in Fig. 8. At C2 and C4 the waveforms are coherent over a significant portion of the Pi2 range and, in addition, the phase difference at frequencies for which the coherence exceeds the threshold is consistently around −90°. Although several phase skips are evident in the phase-time plots, these correlate well with the packet structure of the waveforms plotted in Figs. 4b and d. During the body of the Pi2 event the field components in question are thus in quadrature.

The poloidal mode therefore appears to be standing in both the radial and field-aligned directions, establishing the existence of at least a waveguide mode. The issue of azimuthal propagation will be addressed shortly.

Table 2c reflects the phase of b_ϕ relative to E_ν averaged over the Pi2 band. At both C2 and C4 the condition $\delta(E_\nu, b_\phi)$=90° lies close to the calculated range of uncertainty. The origin of the data in Table 2c is plotted in Fig. 9. It is apparent that E_ν and b_ϕ are coherent with a consistent phase difference over an appreciable portion of the Pi2 range. Furthermore, the phase difference is stable at approximately

Table 2. Average phase differences between orthogonal electric and magnetic field components: **(a)** b_μ versus E_ϕ, **(b)** b_ν versus E_ϕ, **(c)** b_ϕ versus E_ν.

(a)	$\delta(E_\phi, b_\mu)$	$\cos\delta$
C1	93.4°±1.7°	–0.059
C2	−110.7°±2.2°	–0.353
C3		
C4	−114.5°±1.4°	–0.415
(b)	$\delta(E_\phi, b_\nu)$	$\cos\delta$
C1		
C2	−81.4°±6.1°	+0.150
C3		
C4	−93.1°±5.2°	–0.054
(c)	$\delta(E_\nu, b_\phi)$	$\cos\delta$
C1		
C2	98.9°±9.0°	–0.155
C3		
C4	99.2°±3.4°	–0.160

90° for the entire duration of the event. In this case the instantaneous and cross-spectral phase are in accord, providing a persuasive argument for a toroidal mode standing wave.

A discussion of the field-aligned phase relationships at C1 has been deferred until now since the proximity of the satellite to the magnetic equatorial plane results in small amplitudes for the transverse magnetic field components. The amplitude of the electric field, however, is not inconsequential. A field-aligned standing wave at C1 cannot be discounted since these observations are consistent with an odd harmonic standing wave, which has a node in the transverse magnetic field and an antinode in the electric field on the equatorial plane. However, there is additional evidence in support of odd harmonic structure.

Scant coherence at C1 renders the evaluation of $\delta(E_\phi, b_\nu)$ and $\delta(E_\nu, b_\phi)$ using cross-spectral techniques rather unreliable. No estimates are thus given in Table 2. Inspection of the instantaneous phase differences in Figs. 8a and 9a is illuminating. Admitting that there is certainly a degree of mutability in these curves, it is evident that relatively consistent phase relationships $\delta(E_\phi, b_\nu)\sim 90°$ and $\delta(E_\nu, b_\phi)\sim -90°$ are maintained during the event, the most significant departures being due to a node in the wave packet structure at around 18:15 UTC.

The symmetry of a field-aligned standing wave may be determined from the phase of pairs of orthogonal transverse magnetic and electric field perturbations. For an odd harmonic toroidal oscillation a satellite somewhat above the geomagnetic equatorial plane should observe $\delta(E_\nu, b_\phi)\sim -90°$, that is, E_ν leading in phase, while at the same position an even harmonic would have b_ϕ leading in

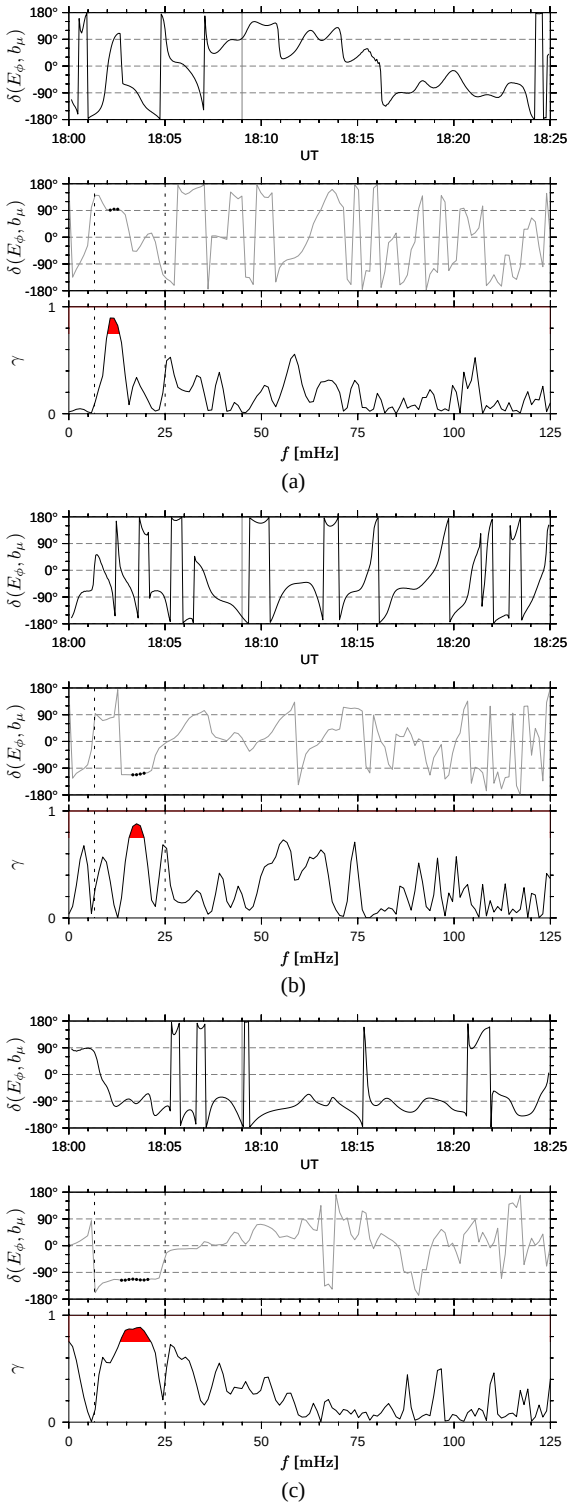

Fig. 7. Coherence and phase difference between b_μ and E_ϕ at **(a)** C1, **(b)** C2, and **(c)** C4. The shaded portions of the coherence curves indicate frequencies for which γ exceeds the threshold of 75%, and at these frequencies solid points are plotted for the phase difference.

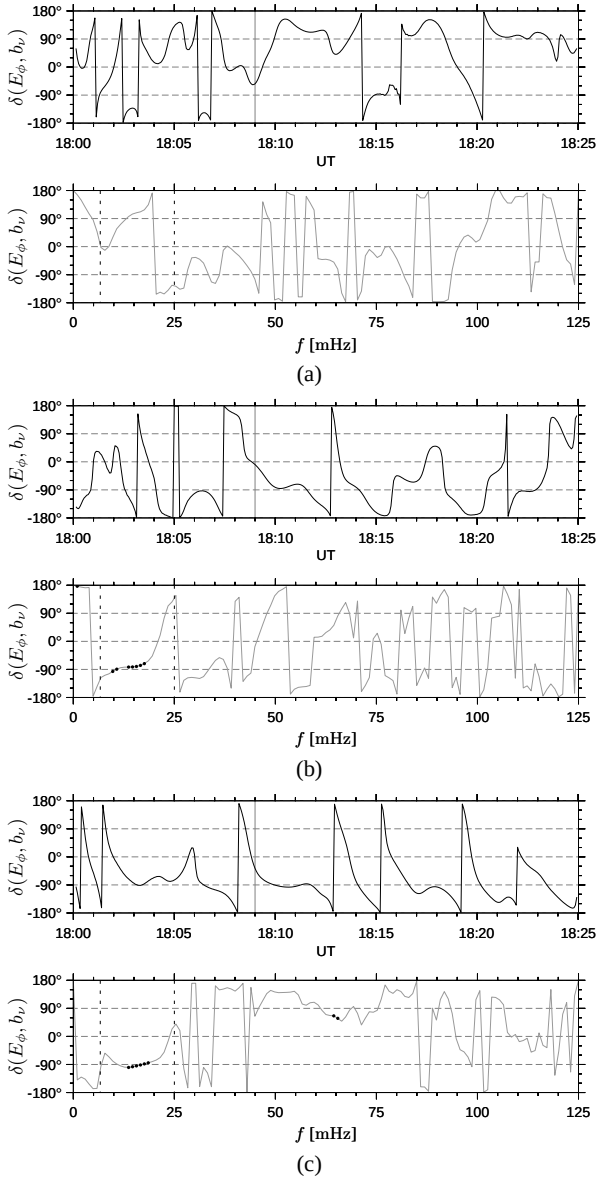

Fig. 8. Phase difference between E_ϕ and b_ν at **(a)** C1, **(b)** C2 and **(c)** C4. Solid points are only plotted at frequencies for which γ exceeds the threshold of 75%.

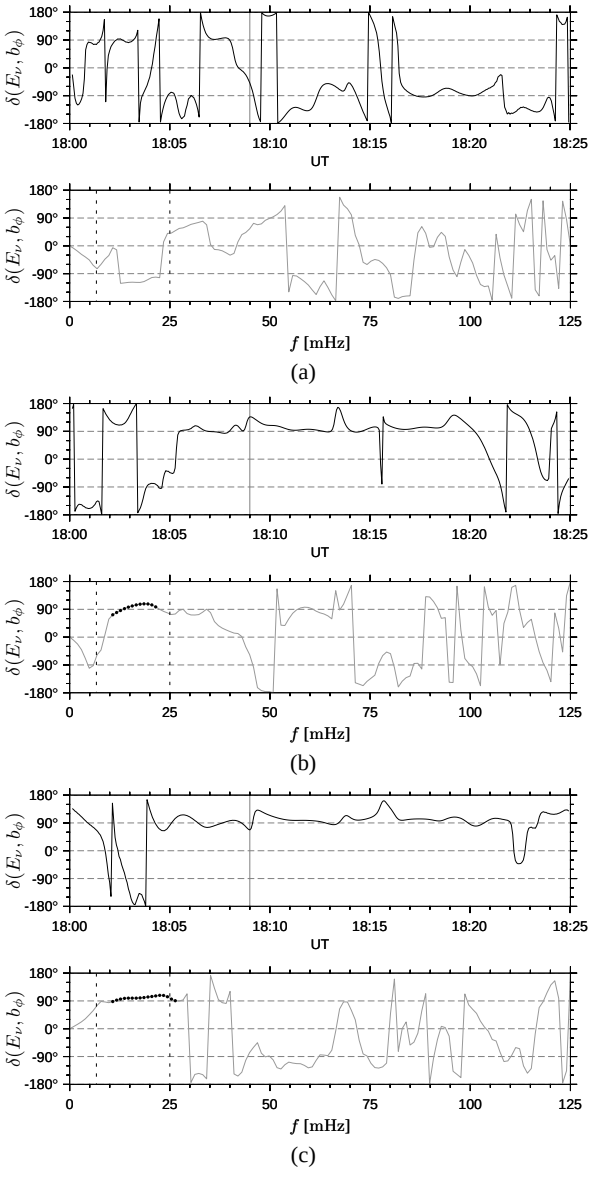

Fig. 9. Phase difference between E_ν and b_ϕ at **(a)** C1, **(b)** C2 and **(c)** C4. Solid points are only plotted at frequencies for which γ exceeds the threshold of 75%.

phase with $\delta(E_\nu, b_\phi) \sim 90°$ (Cummings et al., 1978). The situation is reversed for a satellite located just below the equatorial plane. Similarly, an odd harmonic of the radially transverse wave should have $\delta(E_\phi, b_\nu) = 90°$ or –90° just above or below the equatorial plane respectively (Singer et al., 1982).

The event on 21 January 2003 would have been ideally suited to determining the harmonic order of the field-aligned standing wave since satellites are simultaneously located on either side of the geomagnetic equatorial plane (C1 is in the northern hemisphere at $\lambda = 1.9°$, while C2 and C4 are in the southern hemisphere at $\lambda = -5.9°$ and $-17.0°$, respectively). Unfortunately the coherence at C1 lies below the threshold and phase measurements based on cross-spectral analysis cannot therefore be regarded with conviction. Nevertheless, based on instantaneous phase measurements it has been argued that the phase at C1 may be plausibly assessed. If one is prepared to accept the phase estimates at C1, then these data yield several conclusions: there is a 180° change in phase across the equatorial plane; the phase difference between b_ϕ and E_ν is $-90°$ above and 90° below the equatorial plane; while for b_ν and E_ϕ the corresponding phase differences are 90° and $-90°$, respectively. Altogether these are indicative

of an odd harmonic (symmetric) oscillation. Such an oscillation would arise from an initial disturbance which was symmetric about the equatorial plane.

The fact that the meridional and azimuthal magnetic field perturbations are small at C1 (cf. Fig. 6), which is the satellite located closest to the dipole equatorial plane, supports the contention of an odd harmonic. Disparate conductivities in the northern and southern hemisphere ionospheres may result in the transverse node becoming a "near-node" and its location shifting slightly away from the equatorial plane (Allan, 1982). Since the displacement of the node is small, phase measurements across the equatorial plane are poor diagnostics of asymmetric ionospheric conductivity for odd harmonic waves. The position of the "null-point", where the field-aligned Poynting flux is zero, may be considerably displaced from the equatorial plane, and is thus a more sensitive indicator.

The transport of wave energy within the magnetosphere is an electromagnetic process characterised by the Poynting vector, $\mathbf{\Pi}$. Since the Poynting vector oscillates at a frequency twice that of the underlying waveform, it is more meaningful to examine the time-averaged quantity

$$\langle \mathbf{\Pi} \rangle = \frac{1}{T} \int_0^T \frac{\boldsymbol{E} \times \boldsymbol{b}}{\mu_0} \mathrm{d}t \,,$$

where, for the purposes of Pi2 pulsations, an appropriate integration interval is around 150 s. The calculated Poynting flux is strongly dependent on both the subtraction of the ambient magnetic field and the integration interval. The orientation of $\langle \mathbf{\Pi} \rangle$ with respect to the MFA coordinate axes is furnished in terms of the angles defined in Fig. 10, where α is the polar angle and β the azimuthal angle, the origin of which is in the meridian plane.

Zhu and Kivelson (1989) demonstrated that the cavity mode energy flux is directed towards resonant field lines and that within the plasmasphere the radial component of the Poynting flux may indicate either the inward or outward flow of energy depending on whether the measurement is taken outside or inside the resonant field line.

Poynting vector data are plotted in Fig. 11. Data for C3 are omitted since the full electric field vector was not available for the period of interest. The three components of $\mathbf{\Pi}$ are only included for C2, but the information embodied in the plots for C1 and C4 completely specifies both the magnitude and orientation of the average Poynting flux. The grey curves correspond to the instantaneous components of $\mathbf{\Pi}$ filtered for the Pi2 range, while the black curves are averaged using a sliding 150 s window, and represent the integrated Poynting vector. The transport of electromagnetic energy peaks shortly after the onset of the event.

At C2 the component aligned with the ambient magnetic field has a mean value close to zero. This implies a negligible flow of energy along the field line, which is in agreement with the field-aligned standing wave established earlier. Since the satellite is located below the equatorial plane the small negative excursion during the body of the event may be interpreted as the flow of energy away from the equatorial plane and down towards the ionosphere in the southern hemisphere. The net flux down the field line is also apparent in the fact that $\alpha \gtrsim 90°$ during the event. The conditions at C4, located furthest from the equatorial plane, consistently indicate southward Poynting flux throughout the event. At C1 α is initially around 180°, but during the energy flux maximum is closer to 90°, indicating an insignificant field-aligned flux. The trend in α at C1 may indicate that the satellite traverses the null-point in the field-aligned oscillation during the event, and thus detects the flow of energy towards the southern and northern ionospheres during the initial and final stages of the event respectively.

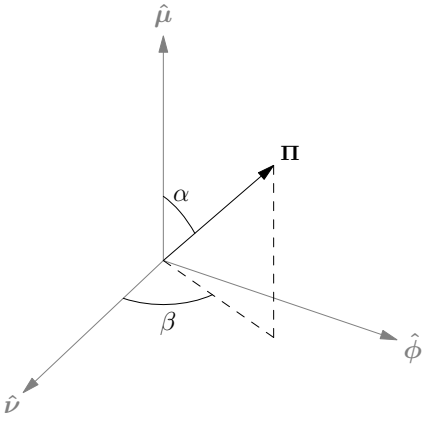

Fig. 10. Angles specifying the orientation of the Poynting vector with respect to the MFA coordinate axes.

The orientation angle β reflects the direction of energy flux in the plane perpendicular to the ambient magnetic field. At both C2 and C4 $\beta \simeq 90°$, which signifies eastward energy flow without any appreciable radial component. Since the satellites are located in the midnight-dawn quadrant this implies that the waves are transporting energy away from midnight. The situation on C1 is more interesting: the Poynting vector appears to be directed westward during the first wave packet and changes to an easterly orientation at the beginning of the second wave packet. During both of these intervals energy is propagating almost exclusively in the azimuthal direction so that, although the argument in favour of a cavity mode at C1 presented earlier on the basis of phase differences was inconclusive, there is clearly minimal radial energy flux. The magnitude of the Poynting flux measured on C1 is appreciably smaller than that on the other satellites.

Waves propagating in a dipole geometry are often assumed to have the form $\exp[j(m\phi - \omega t)]$, where m is the azimuthal wave number. The azimuthal wave number for Pi2 events manifests a pronounced latitudinal dependence, with $|m|$ as large as 20 at high latitudes, but decreasing to less than 1 close to the equator (Yumoto, 1986). Southwood and Stuart

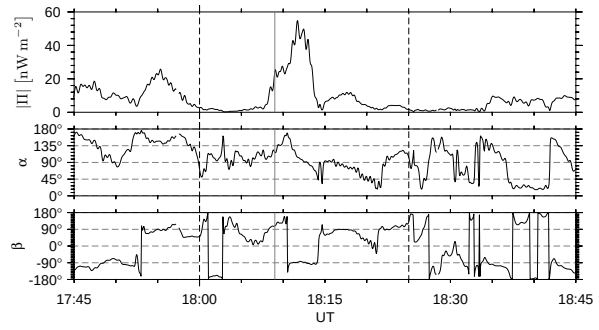

(a)

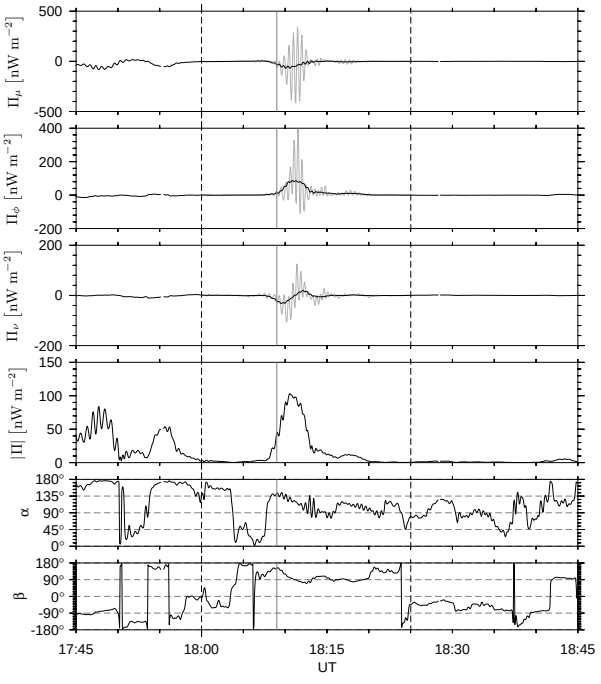

(b)

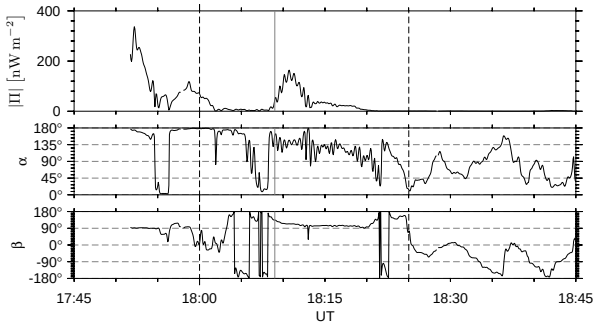

(c)

Fig. 11. Poynting flux at satellites **(a)** C1, **(b)** C2 and **(c)** C4 during the event on 21 January 2003. In (b) each of the components, Π_ν, Π_ϕ and Π_μ, is filtered over the Pi2 frequency range (grey curve) and averaged over a 150 s window (black curve). The Poynting flux magnitude and orientation angles reflect the 150 s average.

(1980) found that the coherence between ground stations was highest in the midnight sector and observed small m, typically $\lesssim$4. Mier-Jedrzejowicz and Southwood (1979) found $|m|\lesssim$6 in the 8–25 mHz band, and $m\sim$2 for a Pi2 event. The lack of any discernible phase lag between Pi2 observations at equatorial latitudes near noon and midnight indicates that $m\sim$0 at low latitudes (Wright, 1994).

An ideal cavity resonance should exhibit no phase advance in the azimuthal direction (Walker et al., 1992). However, as was illustrated previously, there is a definite sense of azimuthal propagation during the event on 21 January 2003 and it is thus possible to evaluate the azimuthal wave number. Estimating m from Cluster data is often not practicable because the error induced by the satellites' limited azimuthal separation can be prohibitively large. However, in this instance the distance between the western and eastern extremities of the constellation allows a reliable estimate.

In Fig. 12 the inter-satellite cross-spectral data for the azimuthal magnetic field are presented. Each panel represents the relationship between the signals on a pair of satellites. The rows correspond to the reference satellite, so that, for instance, the data in the top left panel of Fig. 12b reflects the amount by which the phase at C1 leads that at C2. It is apparent from Fig. 12a that b_ϕ is coherent between C2 and C4 in the Pi2 band. The coherence over this frequency range for the other satellite pairs has a peak but does not surpass the threshold. C2 and C4 are suitable for an estimate of m since they were located at approximately the same L and, in addition, C2 was 2.4° west of C4. The mean phase difference in b_ϕ for the C2-C4 pair is 32.4°. The radial electric field is also coherent between C2 and C4 over the same frequency interval and the mean phase difference is 31.4°.

The above phase difference measurements yield $m\sim+13.7\pm4.8$ and $m\sim+13.3\pm2.0$ for b_ϕ and E_ν, respectively. These relatively large values for m imply an azimuthal wavelength of roughly 2.1 R_E. At a frequency of 17.0 mHz this corresponds to a phase speed of 227 km/s, consistent with a plasma density of around $N\sim10^3\,\mathrm{cm}^{-3}$. Pekrides et al. (1997) found that similar high values of m are excited within the plasmasphere by evanescent barrier penetration, although the disturbance is dominated by waves with smaller m. It should be noted that non-zero m is required for coupling between compressional and toroidal pulsations. Positive m corresponds to eastward phase propagation, which, since the satellites are located in the morning sector, indicates that the waves are travelling towards noon.

5 Conclusions

Observations in space (Takahashi et al., 1995) and at ground stations (Sutcliffe and Yumoto, 1989, 1991) indicate that low latitude Pi2 pulsations are attributable to plasmaspheric cavity mode resonances. Takahashi et al. (2001) observed E_ϕ and b_μ in quadrature within the plasmasphere during a

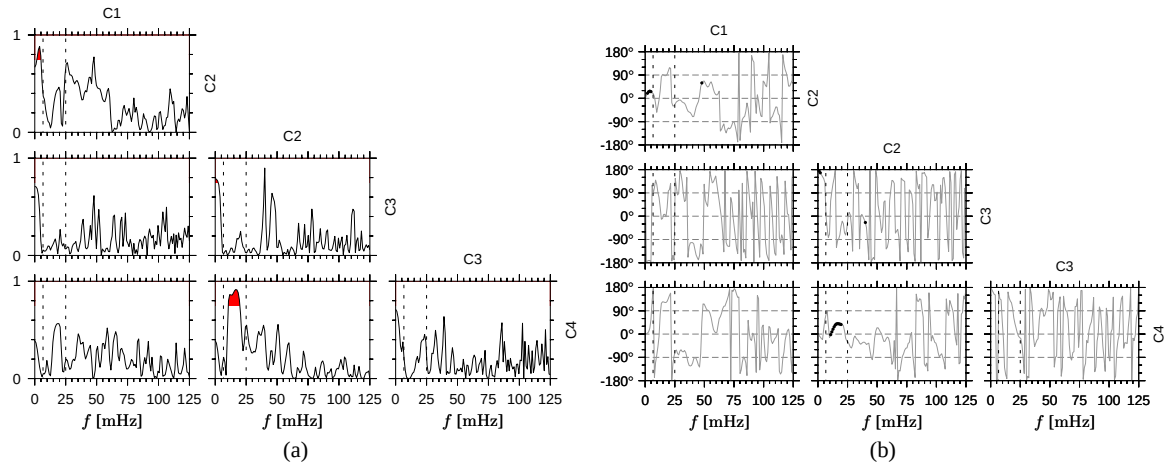

Fig. 12. Inter-satellite **(a)** coherence and **(b)** phase for the azimuthal component of the magnetic field, b_ϕ.

Pi2 event, and concluded that this was evidence of a radial standing wave. Keiling et al. (2001) documented evidence of simultaneous standing poloidal and toroidal waves during a Pi2 event observed on Polar.

During a Pi2 event on 21 January 2003 the Cluster constellation had a serendipitous geometry which placed three satellites within the plasmasphere, while the fourth was located on or just outside the plasmapause. The event was only observed clearly on those three satellites situated within the plasmasphere. At these locations the waves were coherent and exhibited both poloidal and toroidal oscillations. It was possible to determine signatures of a standing wave in the radial direction. Both the transverse magnetic components exhibited characteristics of a field-aligned standing wave, consistent with the observations of Keiling et al. (2001). These observations are strongly suggestive of a cavity mode resonance within the plasmasphere. Specifically, the following observations support a plasmaspheric cavity resonance:

1. a consistent set of discrete frequencies extending upward from the Pi2 range is evident in the compressional spectra at all satellites located within the plasmasphere;
2. the modulus of the phase difference $\delta(E_\phi, b_\mu)$ is close to 90° and therefore indicative of a radial standing wave;
3. the orthogonal electric and magnetic field components corresponding to radially transverse field-aligned waves are in quadrature;
4. there is no consequential net flow of energy parallel to the background magnetic field or in the radial direction.

The relative phase of the electric and magnetic field perturbations associated with the radially transverse standing waves at locations above and below the equatorial plane allow one to infer that these standing waves represent odd harmonics. A toroidal mode standing wave also exists within the plasmasphere, and appears to be an odd harmonic.

The high latitude Pi2 signature is often attributed to transient Alfvén waves on lines of force which map to the auroral oval (Baumjohann and Glaßmeier, 1984; Sutcliffe and Yumoto, 1991). Although the coherence between b_ν and b_ϕ, and the relatively large amplitude of b_ϕ at the satellite outside the plasmasphere suggest that the azimuthal oscillation is a FLR, corroboration from the phase difference $\delta(E_\nu, b_\phi)$ is not available since the radial electric field is not accessible during the entire event. The fact that the onset of coherent activity at C3 precedes that at the remaining satellites by a few minutes is consistent with its location at higher L: the delay at the satellites located within the plasmasphere may be attributed to the time interval required for inward radial propagation.

Consideration of the Poynting flux indicates that only a little energy flows along the field lines, directed towards the nearest ionospheric footprint, where it is presumably dissipated. Azimuthal energy transfer was found to be directed towards noon, which concurs with a source of Pi2 around midnight. This should be contrasted with the observations of Osaki et al. (1998), who found the Poynting flux measured on the Akebono satellite to be directed along the field line towards the closest ionosphere, with negligible ionospheric reflection. However, at the times of the events considered, Akebono was located at smaller L, further from the auroral zone, and thus on field lines mapping to significantly lower ionospheric conductivity. Further observations from the Polar satellite (Keiling et al., 2001) indicate Poynting flux directed outward and eastward. The outward flow of energy was interpreted as indicative of more efficient reflection of compressional waves at the inner boundary. Both Osaki et al. (1998) and Keiling et al. (2001) documented Poynting flux magnitudes significantly larger than those observed here.

Finally, several instances have been presented in which conventional spectral analysis techniques were not ideally suited to the investigation of these transient phenomena. In these situations the merits of the complementary data acquired from the analytical signal are quite apparent. Other methods, such as deconvolution (Behrens and Glaßmeier, 1986), might also be worth exploring.

Acknowledgements. The Cluster FGM data were provided by K.-H. Glaßmeier of the Technical University of Braunschweig, Germany. We acknowledge G. D. Reeves of Los Alamos National Laboratory for providing the geosynchronous particle data, obtained through http://leadbelly.lanl.gov/lanl_ep_data/. The Kakioka and Yinchuan magnetometer data were provided by the World Data Center for Geomagnetism, Kyoto. The collaboration between the University of KwaZulu-Natal and the Royal Institute of Technology is supported by the National Research Foundation (NRF) of South Africa and the Swedish International Development Cooperation Agency (SIDA). Work at the Royal Institute of Technology was partially supported by the Swedish National Space Board and the Alfvén Laboratory Centre for Space and Fusion Plasma Physics. We are grateful to the referees for their cogent and perceptive comments.

Topical Editor I. A. Daglis thanks W. Allan and A. Keiling for their help in evaluating this paper.

References

Akasofu, S.-I.: Polar and Magnetospheric Substorms, vol. 11 of Astrophysics and Space Science Library, D. Reidel, Dordrecht, Holland, 1968.

Akasofu, S.-I. (Ed.): Dynamics of the Magnetosphere, D. Reidel, 1980.

Allan, W.: Phase variation of ULF pulsations along the geomagnetic field-line, Planet. Space Sci., 30, 339–346, 1982.

Allan, W., Poulter, E. M., and White, S. P.: Hydromagnetic wave coupling in the magnetosphere—Plasmapause effects on impulse-excited resonances, Planet. Space Sci., 34, 1189–1200, 1986.

Allan, W., Menk, F. W., Fraser, B. J., Li, Y., and White, S. P.: Are low-latitude Pi2 pulsations cavity/waveguide modes?, Geophys. Res. Lett., 23, 765–768, 1996.

Balogh, A., Dunlop, M. W., Cowley, S. W. H., Southwood, D. J., Thomlinson, J. G., Glassmeier, K. H., Musmann, G., Lühr, H., Buchert, S., Acuña, M. H., Fairfield, D. H., Slavin, J. A., Riedler, W., Schwingenschuh, K., and Kivelson, M. G.: The Cluster Magnetic Field Investigation, Space Sci. Rev., 79, 65–91, 1997.

Baumjohann, W. and Glaßmeier, K.-H.: The transient response mechanism and Pi2 pulsations at substorm onset–Review and outlook, Planet. Space Sci., 32, 1361–1370, 1984.

Behrens, J. and Glaßmeier, K.-H.: Deconvolution as a method for the separation of Pi2 pulsations from background field variations, J. Geophys., 59, 195–201, 1986.

Chen, L. and Hasegawa, A.: A Theory of Long-Period Magnetic Pulsations, 1. Steady State Excitation of Field Line Resonance, J. Geophys. Res., 79, 1024–1032, 1974.

Chi, P. J. and Russell, C. T.: Phase skipping and Poynting flux of continuous pulsations, J. Geophys. Res., 103, 29 479–29 492, 1998.

Cummings, W. D., Deforest, S. E., and McPherron, R. L.: Measurements of the Poynting Vector of Standing Hydromagnetic Waves at Geosynchronous Orbit, J. Geophys. Res., 83, 697–706, 1978.

Escoubet, C. P., Fehringer, M., and Goldstein, M.: The Cluster mission, Ann. Geophys., 19, 1197–1200, 2001, http://www.ann-geophys.net/19/1197/2001/.

Fukunishi, H.: Polarization Changes of Geomagnetic Pi 2 Pulsations Associated With the Plasmapause, J. Geophys. Res., 80, 98–110, 1975.

Glassmeier, K.-H., Buchert, S., Motschmann, U., Korth, A., and Pedersen, A.: Concerning the generation of geomagnetic giant pulsations by drift-bounce resonance ring current instabilities, Ann. Geophys., 17, 338–350, 1999, http://www.ann-geophys.net/17/338/1999/.

Gupta, J. and Stening, R. J.: Some Characteristics of Irregular Micropulsations Pi2 at High Latitude Stations, Can. J. Phys., 49, 2338–2349, 1971.

Gustafsson, G., Boström, R., Holback, B., Holmgren, G., Lundgren, A., Stasiewicz, K., Åhlén, L., Mozer, F. S., Pankow, D., Harvey, P., Berg, P., Ulrich, R., Pedersen, A., Schmidt, R., Butler, A., Fransen, A. W. C., Klinge, D., Thomsen, M., Fälthammar, C.-G., Lindqvist, P.-A., Christenson, S., Holtet, J., Lybekk, B., Sten, T. A., Tanskanen, P., Lappalainen, K., and Wygant, J.: The Electric Field and Wave Experiment for the Cluster Mission, Space Sci. Rev., 79, 137–156, 1997.

Jacobs, J. A., Kato, Y., Matsushita, S., and Troitskaya, V. A.: Classification of Geomagnetic Micropulsations, J. Geophys. Res., 69, 180–181, 1964.

Keiling, A., Wygant, J. R., Cattell, C., Kim, K.-H., Russell, C. T., Milling, D. K., Temerin, M., Mozer, F. S., and Kletzing, C. A.: Pi2 pulsations observed with the Polar satellite and ground stations: Coupling of trapped and propagating fast mode waves to a midlatitude field line resonance, J. Geophys. Res., 106, 25 891–25 904, 2001.

Kepko, L. and Kivelson, M.: Generation of Pi2 pulsations by bursty bulk flows, J. Geophys. Res., 104, 25 021–25 034, 1999.

Kim, K.-H., Takahashi, K., Lee, D.-H., Lin, N., and Cattell, C. A.: A comparison of Pi2 pulsations in the inner magnetosphere and magnetic pulsations at geosynchronous orbit, J. Geophys. Res., 106, 18 865–18 872, 2001.

Kim, K.-H., Takahashi, K., Lee, D.-H., Sutcliffe, P. R., and Yumoto, K.: Pi2 pulsations associated with poleward boundary intensifications during the absence of substorms, J. Geophys. Res., 110, doi:10.1029/2004JA010780,, 2005.

Lanzerotti, L. J., Fukunishi, H., and Chen, L.: ULF Pulsation Evidence of the Plasmapause, 3. Interpretation of Polarisation and Spectral Amplitude Studies of Pc 3 and Pc 4 Pulsations Near $L = 4$, J. Geophys. Res., 79, 4648–4653, 1974.

Lee, D.-H.: Dynamics of MHD wave propagation in the low-latitude magnetosphere, J. Geophys. Res., 101, 15 371–15 386, 1996.

Lee, D.-H.: On the generation mechanism of Pi 2 pulsations in the magnetosphere, Geophys. Res. Lett., 25, 583–586, 1998.

Lin, C. A., Lee, L. C., and Sun, Y. J.: Observations of Pi 2 Pulsations at a Very Low Latitude ($L = 1.06$) Station and Magnetospheric Cavity Resonances, J. Geophys. Res., 96, 21 105–21 113, 1991.

McCormac, B. M. (Ed.): Magnetospheric Physics, D. Reidel, 1974.

McIlwain, C. E.: Coordinates for Mapping the Distribution of Mag-

netically Trapped Particles, J. Geophys. Res., 66, 3681–3691, 1961.

McIlwain, C. E.: Substorm Injection Boundaries, in: Magnetospheric Physics, edited by: McCormac, B. M., 143–154, 1974.

Mier-Jedrzejowicz, W. A. C. and Southwood, D. J.: The East-West structure of mid-latitude geomagnetic pulsations in the 8–25 mHz band, Planet. Space Sci., 27, 617–630, 1979.

Olson, J. V.: Pi2 pulsations and substorm onsets: A review, J. Geophys. Res., 104, 17 499–17 520, 1999.

Olson, J. V. and Rostoker, G.: Pi 2 pulsations and the auroral electrojet, Planet. Space Sci., 23, 1129–1139, 1975.

Osaki, H., Takahashi, K., Fukunishi, H., Nagatsuma, T., Oya, H., Matsuoka, A., and Milling, D. K.: Pi2 pulsations observed from the Akebono satellite in the plasmasphere, J. Geophys. Res., 103, 17 605–17 616, 1998.

Paschmann, G. and Daly, P. W. (Eds.): Analysis Methods for Multi-Spacecraft Data, ESA Publications Division, 1998.

Pekrides, H., Walker, A. D. M., and Sutcliffe, P. R.: Global modeling of Pi 2 pulsations, J. Geophys. Res., 102, 14 343–14 354, 1997.

Potemra, T. A., Lühr, H., Zanetti, L. J., Takahashi, K., Erlandson, R. E., Marklund, G. T., Block, L. P., Blomberg, L. G., and Lepping, R. P.: Multisatellite and ground-based observations of transient ULF waves, J. Geophys. Res., 94, 2543–2554, 1989.

Rostoker, G.: The polarization characteristics of Pi-2 micropulsations and their relation to the determination of possible source mechanisms for the production of nighttime impulsive micropulsation activity, Can. J. Phys., 45, 1319–1335, 1967a.

Rostoker, G.: The Frequency Spectrum of Pi 2 Micropulsation Activity and Its Relationship to Planetary Magnetic Activity, J. Geophys. Res., 72, 2032–2039, 1967b.

Rostoker, G. and Olson, J. V.: Pi 2 Micropulsations as Indicators of Substorm Onsets and Intensifications, J. Geomag. Geoelectr., 30, 135–147, 1978.

Saito, T.: Geomagnetic Pulsations, Space Sci. Rev., 10, 319–412, 1969.

Saito, T., Sakurai, T., and Koyama, Y.: Mechanism of association between Pi2 pulsation and magnetospheric substorm, J. Atmos. Terr. Phys., 38, 1265–1277, 1976.

Sakurai, T. and McPherron, R. L.: Satellite Observations of Pi 2 Activity at Synchronous Orbit, J. Geophys. Res., 88, 7015–7027, 1983.

Samson, J. C., Jacobs, J. A., and Rostoker, G.: Latitude-Dependent Characteristics of Long-Period Geomagnetic Micropulsations, J. Geophys. Res., 76, 3675–3683, 1971.

Shiokawa, K., Baumjohann, W., Haerendel, G., Paschmann, G., Fennell, J. F., Friis-Christensen, E., Lühr, H., Reeves, G. D., Russell, C. T., Sutcliffe, P. R., and Takahashi, K.: High-speed ion flow, substorm current wedge, and multiple Pi 2 pulsations, J. Geophys. Res., 103, 4491–4508, 1998.

Singer, H. J., Hughes, W. J., and Russell, C. T.: Standing Hydromagnetic Waves Observed by ISEE 1 and 2: Radial Extent And Harmonic, J. Geophys. Res., 87, 3519–3529, 1982.

Singer, H. J., Hughes, W. J., Fougere, P. F., and Knecht, D. J.: The localization of Pi 2 pulsations: Ground-satellite observations, J. Geophys. Res., 88, 7029–7036, 1983.

Southwood, D. J. and Stuart, W. F.: Pulsations at the Substorm Onset, in: Dynamics of the Magnetosphere, edited by: Akasofu, S.-I., 341–355, 1980.

Stuart, W. F.: A mechanism of selective enhancement of Pi 2's by the plasmasphere, J. Atmos. Terr. Phys., 36, 851–859, 1974.

Stuart, W. F. and Barsczus, H. E.: Pi's observed in the daylight hemisphere at low latitudes, J. Atmos. Terr. Phys., 42, 487–497, 1980.

Stuart, W. F. and Booth, D. C.: A study of the power spectra of dPi's and Pi 2's, J. Atmos. Terr. Phys., 36, 835–849, 1974.

Sutcliffe, P. R.: Improved Resolution in Pi2 Magnetic Pulsation Power Spectra, Planet. Space Sci., 22, 1461–1470, 1974.

Sutcliffe, P. R.: The association of harmonics in Pi2 power spectra with the plasmapause, Planet. Space Sci., 23, 1581–1587, 1975.

Sutcliffe, P. R.: Observations of Pi2 pulsations in a near ground state magnetosphere, Geophys. Res. Lett., 25, 4067, 1998.

Sutcliffe, P. R. and Yumoto, K.: Dayside Pi 2 pulsations at low latitudes, Geophys. Res. Lett., 16, 887–890, 1989.

Sutcliffe, P. R. and Yumoto, K.: On the cavity mode nature of low-latitude Pi 2 pulsations, J. Geophys. Res., 96, 1543–1551, 1991.

Takahashi, K., Ohtani, S.-I., and Anderson, B. J.: Statistical analysis of Pi 2 pulsations observed by the AMPTE CCE spacecraft in the inner magnetosphere, J. Geophys. Res., 100, 21 929–21 941, 1995.

Takahashi, K., Ohtani, S.-I., Hughes, W. J., and Anderson, R. R.: CRRES observation of Pi2 pulsations: Wave mode inside and outside the plasmasphere, J. Geophys. Res., 106, 15 567–15 582, 2001.

Takahashi, K., Lee, D.-H., Nosé, M., Anderson, R. R., and Hughes, W. J.: CRRES electric field study of the radial mode structure of Pi2 pulsations, J. Geophys. Res., 108, doi:10.1029/2002JA009761, 2003.

Walker, A. D. M., Ruohoniemi, J. M., Baker, K. B., Greenwald, R. A., and Samson, J. C.: Spatial and Temporal Behavior of ULF Pulsations Observed by the Goose Bay HF Radar, J. Geophys. Res., 97, 12 187–12 202, 1992.

Waters, C. L., Takahashi, K., Lee, D.-H., and Anderson, B. J.: Detection of ultralow-frequency cavity modes using spacecraft data, J. Geophys. Res., 107, doi:10.1029/2001JA000224, 2002.

Webb, D. C.: The analysis of non stationary data using complex demodulation, Ann. Télécommunic., 35, 131–137, 1979.

Welch, P. D.: The Use of Fast Fourier Transform for the Estimation of Power Spectra: A Method Based on Time Averaging Over Short, Modified Periodograms, IEEE Trans. Audio Electroacoust., 15, 70–73, 1967.

Wright, A. N.: Dispersion and wave coupling in inhomogeneous MHD waveguides, J. Geophys. Res., 99, 159–167, 1994.

Yeoman, T. K., Lester, M., Milling, D. K., and Orr, D.: Polarization, propagation and MHD wave modes of Pi2 pulsations: SABRE/SAMNET results, Planet. Space Sci., 39, 983–998, 1991.

Yumoto, K.: Generation and propagation mechanisms of low-latitude magnetic pulsations–A review, J. Geophys., 60, 79–105, 1986.

Zhu, X. and Kivelson, M. G.: Global Mode ULF Pulsations in a Magnetosphere with a Nonmonotonic Alfvén Velocity Profile, J. Geophys. Res., 94, 1479–1485, 1989.